MULTIFRAGMENTATION IN THE REACTION $^{32}S + {}^{58}Ni$ AT 30 AMeV*

A. SIWEK[1], A. BUDZANOWSKI[1], H. FUCHS[2], H. HOMEYER[2], W. KANTOR[1], G. PAUSCH[2], G. ROESCHERT[2], C. SCHWARZ[2], A. SOURELL[2], W. TERLAU[2] AND A. TUTAY[2]

[1]Institute of Nuclear Physics
Radzikowskiego 152, PL-31-342 Kraków, Poland
[2]Hahn-Meitner-Institut
39 Glienicker Str. 100, Berlin, Germany

(Received October 27, 1993)

Processes with high energy dissipation in 30 MeV/A $^{32}S + {}^{58}Ni$ reaction were studied. Coincidences between three intermediate mass fragments (IMF, $Z > 2$) were used to investigate the mechanism of the multifragmentation process. The mass and the velocity distributions of one of the three fragments and the angular correlation between two of them were extracted from the experimental data and compared with predictions of two models for the direct statistical multifragmentation and with the simulations of two sequential binary fissions. The results suggest that the measured three-IMF events determine a mixture of the simultaneous and the sequential processes with the significant domination of the latter.

PACS numbers: 25.70. Gh, 25.70. Np

1. The experiment

The experiments made in HMI in Berlin with the multi-detector array ARGUS were devoted to a study of highly dissipative processes in the reaction $^{32}S + {}^{58}Ni$ at 960 MeV (30A MeV). In this experiment the ARGUS detector consisted of 123 phoswich type detectors and 3 additional semiconductor detectors which served as independent triggers of our registration system. With the semiconductor detectors we measured the energy and

* Presented at the XXIII Mazurian Lakes Summer School on Nuclear Physics, Piaski, Poland, August 18–28, 1993.

the time-of-flight of fragments which allow us to determine their masses. In phoswich detectors projectile-like fragments were identified up to charge $Z = 16$. Additionally, a class of fragments with charge $Z > 2$ and low velocity (stopped in 0.1mm Pilot-U scintillator) was selected — we denote these fragments as HSF (heavy slow fragments).

2. The multifragmentation

To study multifragmentation processes we selected the events with three heavy fragments. One, with the mass $M > 10$ a.m.u. and the velocity $V < 4$ cm/ns denoted IMF1, registered in one of the semiconductor detectors, has by definition the azimuthal angle $\varphi_1 = 0°$. The other two, denoted IMF2 and IMF3, were HSF's registered in phoswich detectors with azimuthal angles defined so that $\varphi_2 < \varphi_3$ (Fig. 1). From these events the distributions of the following observables were extracted:

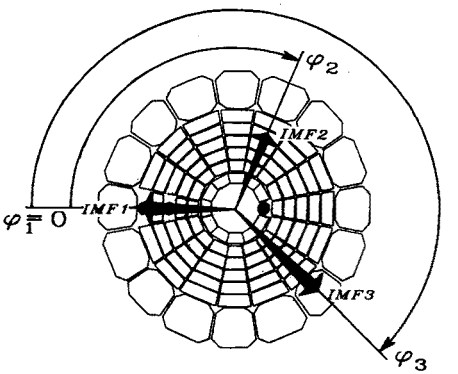

Fig. 1. The definition of the azimuthal angles for the three intermediate mass fragments events (multifragmentation). The IMF1 is registered in one of the three semiconductor trigger detectors and, by definition, has the azimuthal angle $\varphi_1 = 0°$. The IMF2 and IMF3 are registered in the phoswich array and their azimuthal angles are defined so that $\varphi_2 < \varphi_3$ in the anti-clockwise direction.

- mass and velocity of the fragments registered in semiconductor detectors,
- relative azimuthal angle between the heavy fragment registered in a semiconductor detector, and one of the HSF's,
- polar angle of one of the HSF's.

The data were compared with the predictions of two statistical multifragmentation models — the Berlin group [1] model (GROSS) and the Copenhagen group [2] model (CRACKER) — and with simulations of a sequential fission process (SMF).

3. Models

Statistical multifragmentation (or simultaneous break-up) models are based on properties of nuclear matter. Generally it is assumed that after initial compression due to the collision the nucleus expands and enters a regime of low density and mechanical instability, where many fragments of different size are produced simultaneously. The starting point of the calculations is the moment when a fully equilibrated compound nucleus with definite excitation energy, mass and charge is formed. As an output the theories yield velocities, masses and directions of all fragments produced in this process. The serious problem was to determine the initial conditions for the hot compound nucleus (E^*, A, Z). Because in this reaction the dominant process leading to the formation of a hot nucleus is the incomplete fusion we decided to make the calculations for the set of different compound nuclei specified in Table I. The excitation energy was calculated with the

TABLE I

The input channel properties used for calculations of the statistical multifragmentation models. Following quantities are shown: The chemical symbol of the compound nucleus formed in an incomplete fusion (CN), the linear momentum transfer (LMT), the corresponding excitation energy (E^*) and the fraction of the total, cross section f used as a weight for adding contributions from different compound nuclei.

Nr	CN	LMT [%]	E^*[MeV]	f [%]
1	^{62}Zn	12.5	109	37.62
2	^{66}Ge	25.0	200	12.02
3	^{70}Se	37.5	281	8.99
4	^{74}Kr	50.0	357	8.21
5	^{78}Sr	62.5	423	7.77
6	^{82}Zr	75.0	482	6.49
7	^{85}Nb	84.4	522	8.70
8	^{89}Tc	97.0	581	10.37

massive transfer assumption. For each incomplete fusion reaction the three-fragment events were selected and filtered with the detector acceptance. The contributions from each compound nucleus were added with the weights f (see Table I). These weights were obtained from the distribution of the absolute incomplete-fusion cross section over the excitation energy of product nuclei calculated with the help of the semi-microscopic model of projectile break-up and capture, proposed by Möhring *et al.* [3]. The sequential fission assumes that a highly excited nucleus decays through a chain of subsequent fissions or evaporations. We assumed that a compound nucleus formed in an

incomplete fusion reaction evaporates neutrons and light charged particles, the number of which depends on the initial excitation energy. After the evaporation, two independent asymmetric fissions occur. For this scenario simple computer simulations were made in order to check whether one can find a reasonable set of input parameters which allow to reproduce the experimental data. The main ingredients of the simulations are listed below — the free parameters varied to get the best agreement with the experimental data are indicated in the brackets $\langle \ldots \rangle$. All directions are chosen with spatial isotropy.

- As a result of an incomplete fusion reaction the primary compound nucleus is formed. The velocity V_{cn} of this nucleus is chosen randomly with a Gaussian distribution $\langle V^{\circ}_{\mathrm{cn}}, \sigma_{\mathrm{cn}} \rangle$. The mass M_{cn} and the excitation energy E^* are then calculated from the momentum and energy conservation law.
- The primary compound nucleus de-excites by evaporation of light particles. The mass M of the evaporation residues is chosen randomly with the gaussian distribution $\langle M_0, \sigma_M \rangle$.
- The recoil velocity of the compound nucleus V_{er}, caused by the light particle evaporation, is chosen randomly with a Maxwellian distribution. The width of the distribution depends on the mass and excitation energy of the primary compound nucleus and on the number of evaporated particles.
- After evaporation two subsequent fissions occur. The mass asymmetry A_1 of the first fission is chosen randomly with the inverted gaussian distribution $\langle \sigma_1 \rangle$. The velocities of both fragments are calculated according to the Viola systematics. The actual kinetic energy E_{vv} is chosen randomly with a gaussian distribution centered at E_{Vio} and the width $\langle \sigma_{vv} \rangle$.
- The asymmetry factor for the second fission A_2, $\langle \sigma_2 \rangle$ and the velocities of the fission fragments are chosen in the same way.
- All three-fragment events, generated in the way described above, are filtered with the detector acceptance.

4. Results

It was reported earlier [4] that a relative-angle distribution can be used to distinguish between two decay mechanisms. The results of our calculations show only a moderate difference between the predictions of simultaneous break-up and sequential fission, the experiment slightly favouring the latter (Fig. 2a,b). A similar situation is observed for the polar-angle distribution of HSF's (Fig. 3a,b).

A significant difference between the models can be observed in mass and velocity distributions. Both theories of statistical multifragmentation yield

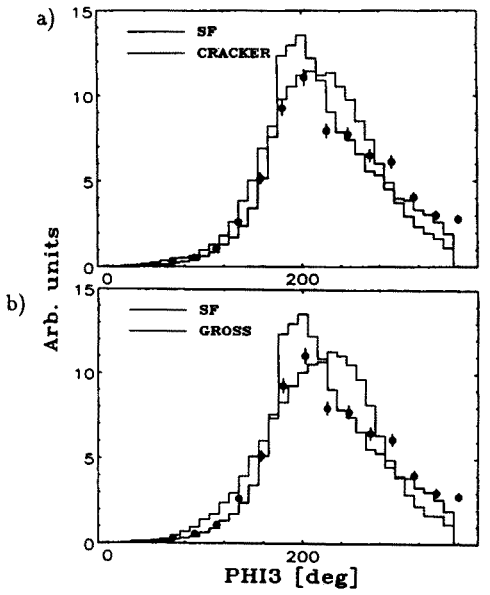

Fig. 2

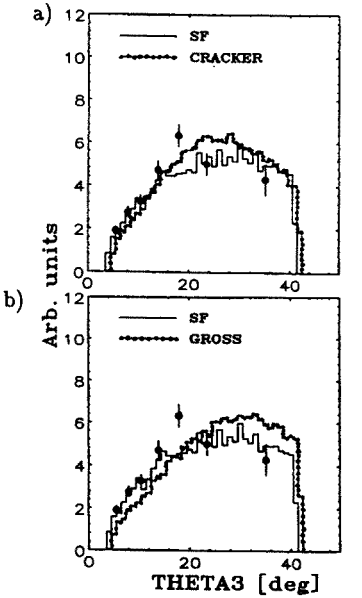

Fig. 3

Fig. 2. The azimuthal angle distribution of the IMF3 registered in coincidence with IMF1 at 23.5° (see Fig. 1), integrated over the azimuthal angle range of the IMF2, $0° < \varphi_2 < 180°$, and over the polar angle range of the IMF2, $8° < \Theta_2 < 41.5°$. a) The comparison of the results of the CRACKER and SMF calculations with the experimental data. b) The comparison of the results of the GROSS and SMF calculations with the experimental data.

Fig. 3. The polar angle distribution of the IMF3 registered in coincidence with IMF1 at 23.5° (see Fig. 4), integrated over the full range of the azimuthal angles φ_2 and φ_3 a) The comparison of the results of the CRACKER and SMF calculations with the experimental data. b) The comparison of the results of the GROSS and SMF calculations with the experimental data.

events with too low masses — only up to about 35 a.m.u. — but can very well reproduce the mass distribution in the region 10–20 a.m.u. (Fig. 4a,b). In contrast to the statistical models, the sequential fission scenario describes the whole mass region above 20 a.m.u. perfectly but underestimates the distribution below this mass (Fig. 4a,b). The velocity distributions calculated with both statistical models have the maximum in the region of 2.7 cm/ns (the center of mass velocity) and are not able to describe the experimental data at all (Fig. 5a,b). The sequential fission simulations give significantly better description, however, the maximum is also at too high a velocity (Fig. 5a,b).

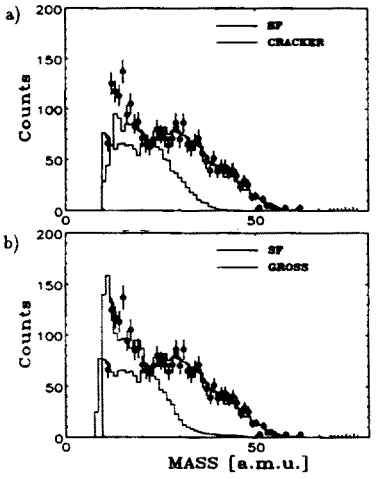

Fig. 4

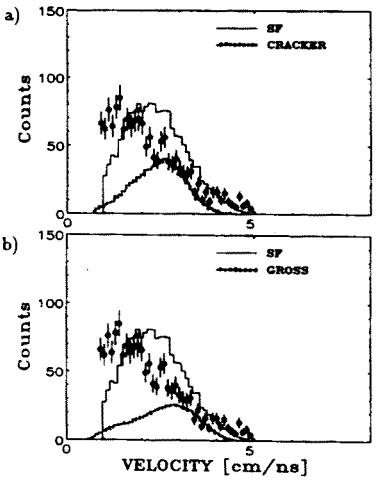

Fig. 5

Fig. 4. The mass distribution of the IMF1 registered at 23.5°, in coincidence with two other IMF's detected in ARGUS. a) The comparison of the results of the CRACKER and SMF calculations with the experimental data. b) The comparison of the results of the GROSS and SMF calculations with the experimental data.

Fig. 5. The velocity distribution of the IMF1 (see Fig. 4), registered at 23.5° in coincidence with two other IMF's detected in ARGUS. a) The comparison of the results of the CRACKER and SMF calculations with the experimental data. b) The comparison of the results of the GROSS and SMF calculations with the experimental data.

5. Conclusions

The experimental data obtained in the present experiment were compared with the predictions of the two statistical multifragmentation models and a sequential fission simulation. The data are better reproduced by the sequential fission scenario than by the simultaneous break-up models. In statistical multifragmentation models we did not use any free parameters and one can presume that changing, for example, the freeze-out volume or excitation energy of the primary compound nuclei one could obtain better results. However, a more detailed analysis shows that these models are not able to yield enough events in the 35–50 a.m.u. mass region. The calculations suggest that the emission of three heavy fragments is a mixture of the two processes with significant domination of the sequential fission process. This is most apparent in the Fig. 4b — one can see that a corresponding mixture can fit the data very well.

REFERENCES

[1] D. Gross, H. Massmann, *Nucl. Phys.* **A443**, 339c (1985).
[2] J.P. Bondorf, R. Donangelo, I.N. Mishustin, H. Schulz, *Nucl. Phys.* **A443**, 321 (1985) .
[3] K. Möhring, D. Gross, T. Srokowski, *Nucl. Phys.* **A533**, 333 (1991) .
[4] J.A. Lopez, J. Randrup, *Nucl. Phys.* **A491**, 477 (1989).